

High sensitivity CIP2A detection for oral cancer using a rapid transistor-based biosensor module F

Cite as: J. Vac. Sci. Technol. B **41**, 013201 (2023); <https://doi.org/10.1116/6.0002175>

Submitted: 24 August 2022 • Accepted: 31 October 2022 • Published Online: 13 December 2022

 Minghan Xian, Jenna L. Stephany,  Chan-Wen Chiu, et al.

COLLECTIONS

Paper published as part of the special topic on [Honoring Dr. Gary McGuire's Research and Leadership as Editor of the Journal of Vacuum Science & Technology for Three Decades](#)

F This paper was selected as Featured



View Online



Export Citation



CrossMark

ARTICLES YOU MAY BE INTERESTED IN

[Overview of atomic layer etching in the semiconductor industry](#)

Journal of Vacuum Science & Technology A **33**, 020802 (2015); <https://doi.org/10.1116/1.4913379>


[Fast SARS-CoV-2 virus detection using disposable cartridge strips and a semiconductor-based biosensor platform](#)

Journal of Vacuum Science & Technology B **39**, 033202 (2021); <https://doi.org/10.1116/6.0001060>


[Accurate quantification of lattice temperature dynamics from ultrafast electron diffraction of single-crystal films using dynamical scattering simulations](#)

Structural Dynamics **9**, 064302 (2022); <https://doi.org/10.1063/4.0000170>





HIDEN
ANALYTICAL



40 YEARS
1982-2022

Instruments for Advanced Science

■ Knowledge,
■ Experience,
■ Expertise

Click to view our product catalogue

Contact Hiden Analytical for further details:
www.HidenAnalytical.com
info@hideninc.com

Gas Analysis

- ▶ dynamic measurement of reaction gas streams
- ▶ catalysis and thermal analysis
- ▶ molecular beam studies
- ▶ dissolved species probes
- ▶ fermentation, environmental and ecological studies

Surface Science

- ▶ UHV TPD
- ▶ SIMS
- ▶ end point detection in ion beam etch
- ▶ elemental imaging - surface mapping

Plasma Diagnostics

- ▶ plasma source characterization
- ▶ etch and deposition process reaction kinetic studies
- ▶ analysis of neutral and radical species

Vacuum Analysis

- ▶ partial pressure measurement and control of process gases
- ▶ reactive sputter process control
- ▶ vacuum diagnostics
- ▶ vacuum coating process monitoring

High sensitivity CIP2A detection for oral cancer using a rapid transistor-based biosensor module F

Cite as: J. Vac. Sci. Technol. B **41**, 013201 (2023); doi: [10.1116/6.0002175](https://doi.org/10.1116/6.0002175)

Submitted: 24 August 2022 · Accepted: 31 October 2022 ·

Published Online: 13 December 2022



Minghan Xian,^{1,a)} Jenna L. Stephany,² Chan-Wen Chiu,¹ Chao-Ching Chiang,¹ Fan Ren,¹ Cheng-Tse Tsai,³ Siang-Sin Shan,³ Yu-Te Liao,³ Josephine F. Esquivel-Upshaw,² and Stephen J. Pearton⁴

AFFILIATIONS

¹Department of Chemical Engineering, University of Florida, Gainesville, Florida 32611

²Department of Restorative Dental Sciences, University of Florida, Gainesville, Florida 32610

³Department of Electrical and Computer Engineering, National Yang Ming Chiao Tung University, Hsinchu 30010, Taiwan

⁴Department of Materials Science and Engineering, University of Florida, Gainesville, Florida 32611

Note: This paper is a part of the Special Topic Collection Special Topic Collection Honoring Dr. Gary McGuire's Research and Leadership as the Editor of the Journal of Vacuum Science & Technology for Three Decades.

^{a)}Electronic mail: mxian@ufl.edu

ABSTRACT

Oral squamous cell carcinoma (OSCC) is one of the most common lip and oral cavity cancer types. It requires early detection via various medical technologies to improve the survival rate. While most detection techniques for OSCC require testing in a centralized lab to confirm cancer type, a point of care detection technique is preferred for on-site use and quick result readout. The modular biological sensor utilizing transistor-based technology has been leveraged for testing CIP2A, and optimal transistor gate voltage and load resistance for sensing setup was investigated. Sensitivities of 1×10^{-15} g/ml have been obtained for both detections of pure CIP2A protein and HeLa cell lysate using identical test conditions via serial dilution. The superior time-saving and high accuracy testing provides opportunities for rapid clinical diagnosis in the medical space.

Published under an exclusive license by the AVS. <https://doi.org/10.1116/6.0002175>

I. INTRODUCTION

Oral cancer is the 13th most common cancer globally, with oral squamous cell carcinoma (OSCC) making up over 90% of oral cancers. An estimated 300 000 new cases and 145 000 deaths worldwide were attributed to oral cancer in 2012. Occurring in one of the most accessible anatomical sites of the body, oral cancer can be easily and quickly detected and treated. When caught early, oral cancers that are still localized and measuring 2 cm or less can be cured with 5-year survival rates exceeding 90%.¹ Visual screening, toluidine blue staining,¹ chemiluminescence, autofluorescence, exfoliative cytology, biopsy/histopathology, and saliva analysis are all currently available oral cancer screening techniques used for early detection.^{1–3} Unfortunately, the nature of these tests is expensive, time-consuming, and labor-intensive while being plagued with low sensitivity and lack of specificity.^{1–4} Saliva analysis and brush biopsies have offered a wealth of opportunities in oral cancer screening.² However, still, there is a need for a more accessible version of a test for immediate response.

Cell proliferation regulating inhibitor of protein phosphatase 2A (p90/CIP2A) has been determined as a biomarker for OSCC.^{3–5} CIP2A is highly expressed in OSCC cell lines and dysplastic and malignant human oral epithelial tissues but not in normal controls.^{6–8} CIP2A is a protein that binds to and inhibits PP2A, a tumor suppressor.^{5,6} The inhibition of PP2A supports cellular transformation through increased cell proliferation.^{6,9} While CIP2A is pronounced in most cancers such as lung¹⁰ and gastric cancer, it is more pronounced in oral cancer.^{11–15} For saliva analysis of CIP2A, enzyme-linked immunoassay (ELISA) test kits are widely available and immunosensors made of carbon nanotubes have begun to develop.⁴ ELISA test kits are restricted to laboratory use, time-consuming, costly, and only have a detection range of 0.156–10 ng/ml.¹⁶ Ding *et al.* created carbon nanotubes with a detection limit of 4.69 pg/ml for CIP2A Ag in a buffer. This sensing technology is expensive, not straightforward, requires analysis, and is an electrochemical method not accessible to a dental office. Nanotubes are also very expensive and, therefore, not cost-effective compared

to the ELISA test and biopsy. Unfortunately, the nature of these tests is expensive, time-consuming, and labor-intensive while having low sensitivity and lack specificity.^{1–4} Saliva analysis and brush biopsies have offered a wealth of opportunities in oral cancer screening.² An accessible and developed CIP2A biosensor with high sensitivity and faster sensing time could be of significant value towards further developing oral cancer screenings in the office.

A low-cost sensor similar to a glucose detection strip has been created as a modular biosensor system consisting of an Si-MOSFET digital reader combined with externalized cartridge sensor strips functionalized for the SARS-CoV-2 virus.^{17–19} The device utilizes the easily accessible glucose test strips to create sensor strips with an Au-plated electrode. This system has also been used to detect cerebrospinal fluid,²⁰ cardiac troponin I, and Zika virus leading to the potential for the CIP2A protein.^{21–23}

In this work, the modular biosensor system has been functionalized to detect CIP2A. The sensitivity has been checked using CIP2A protein dilutions and tested with HeLa cancer cell lysate. We hereby report our first cancer detection study using a similar MOSFET-based sensing system detecting oral cancer biomarker CIP2A with down to femtograms of superior sensitivity compared to previous literature. In addition to pure antigen, HeLa cell lysate is used as a positive control to verify the sensitivity of our system against other proteins and cellular constituents for the first time.

II. EXPERIMENT

The biofunctionalized sensors were made using commercially available glucose test strips. This method for functionalizing these strips follows the method previously used for SARS-CoV-2 virus biosensor strips by Xian *et al.*^{18,19} A general photograph of the sensor circuit and strip as well as schematic diagram for the sensor system is shown in Fig. 1. The test strip's carbon electrodes, located within the microfluidic channel, were gold plated using a 24 K gold plating solution (Gold Plating Services). The Au-plated electrodes were treated with 10 mM thioglycolic acid (TGA) in ethanol for 4h. Next, the TGA functionalized electrodes were immersed in 0.1 mM *N,N'*-dicyclohexylcarbodi-imide in acetonitrile for 1 h. Then, the electrodes were submerged in 0.1 mM *N*-hydroxysuccinimide in acetonitrile for 1 h to complete the two-step chemical reaction for enhancing antibody binding. The excess reactant was removed by rinsing with acetone and DI water. Monoclonal CIP2A antibody 2G10-3B5 (Santa Cruz Biotechnology) was used to functionalize the test strips. The antibody was diluted to 20 $\mu\text{g}/\text{ml}$ in PBS, inserted into the microfluidic channel of the test strips, and then incubated for 18 h at 4 °C. Finally, the test strips were rinsed with phosphate-buffered solution (PBS) and stored at 4 °C in PBS. For testing, HeLa Cell Lysate (Santa Cruz Biotech) and CIP2A Protein (MyBioSource) were serially diluted in PBS and stored at 4 °C. The use of a CIP2A protein with a known concentration allowed us to determine the limit of detection of our sensor for this cancer biomarker. Validation of antibody functionalization using identical methods was demonstrated in current-voltage and capacitance measurements in previous work.^{18,20}

Asynchronous voltage pulse signal was sent to both the gate and drain electrodes of the MOSFET using a printed circuit board designed to use the double-pulse method previously

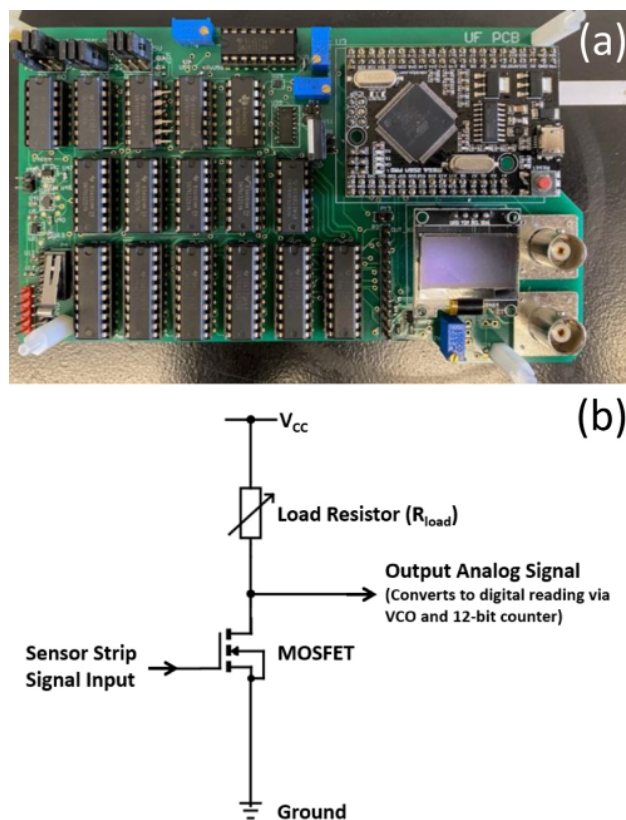


FIG. 1. Photograph of the circuit board (a) and schematic of the sensor circuit (b).

developed.^{18,24–26} Using the same settings as Xian *et al.*,^{17,19,20} the drain pulse duration was around 1.1 ms at a constant voltage. The gate pulse started at 40 μs after the start of the drain pulse signal and stopped at 40 μs before the end. A 15 k Ω resistor connects to the drain as a load resistor. The circuit board generates pulse signals and converts the analog drain output of the MOSFET into a four-digit digital output after each pulse signal using a voltage-controlled oscillator (VCO) (SN74S124N) and a built-in Arduino microcontroller. A built-in LCD screen displays the result on the board. Ten pulse signals are collected and averaged for each measurement for the analog signal and digital readout. An Agilent InfiniiVision DSO7054B oscilloscope collects the analog drain waveform (V_D), and a voltage reading at 750 μs value of the analog waveform was taken for the analog reading.¹⁸

III. RESULTS AND DISCUSSION

The sensing system was fine-tuned to obtain the desired analog waveform before sensing the desired antigen. A proper analog drain voltage, which is the voltage between the MOSFET drain side and the load resistor, is required to meet the minimum input voltage of the VCO, consequently resulting in a sensible digital output. In this sensing setup, the analog output was mainly

affected by two parameters, MOSFET gate voltage and load resistor. The gate voltage and load resistances have been investigated to determine ideal conditions. Figure 2(a) shows time-dependent MOSFET drain waveforms for varying gate voltages (V_G) at a fixed concentration of HeLa cells 1×10^{-5} g/ml at dilution. To mimic sensor performance when testing cells, diluted HeLa cell lysate is

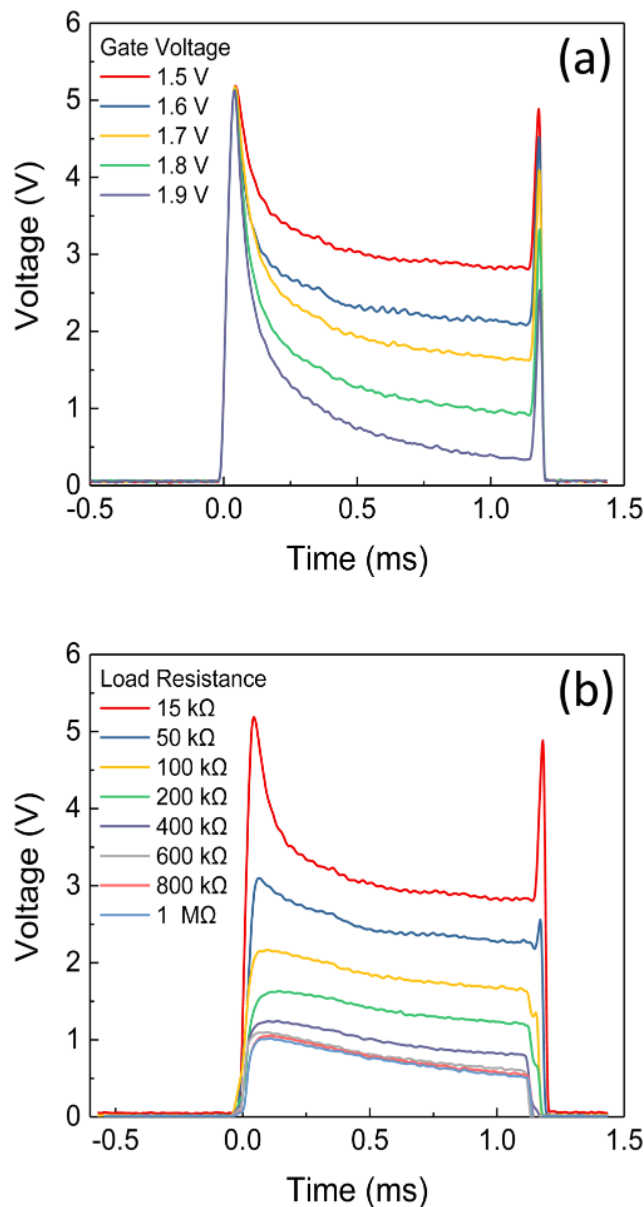


FIG. 2. Analog waveform for sensor output (read between MOSFET drain and load resistor) as a function of the gate voltage applied on MOSFET (a) and load resistance of pull-up resistor (b).

used in this test instead of pure CIP2A. Above a V_G of 1.6 V, the drain voltage was subsequently reduced due to reduced channel conductance. Analog drain voltage with V_G of below 1.6 V was below the required minimum input voltage for the VCO, and no digital sensitivity could be attained. 1.5 V is chosen for optical V_G for sensing since the higher V_D with this gate voltage can produce a reasonable digital output (between the circuit board minimum of around 1700 to a maximum of 3400). Time-dependent MOSFET V_D waveforms were also taken at the same fixed concentration for varying load resistances (R_{load}) at 1.5 V V_G [Fig. 2(b)]. The resulting dynamic sensing waveform continues to flatten and subside with increasing load resistance, typically resulting in reduced or complete loss of sensitivity. The dynamic shape of the analog waveform is caused by the input capacitance of the MOSFET and, therefore, is also strongly dependent on the antigen-antibody interaction of the sensor strip.²⁰ The self-assembled antibody layer interacts with antigen present in solution resulting in spatial and temporal motion in protein structure.^{22,27,28} Furthermore, previous work has shown that different levels of antigen present can directly cause variation in small-signal capacitance of the sensor strip of a similar setup, which is directly connected to the gate of MOSFET.²⁰ Figure 2 shows that the ideal load resistance (R_{load}) is around 15 k Ω , which would result in a significant change in analog and digital output while maintaining proper sensitivity. Note that tuning the V_G and R_{load} is needed for the sensor strips functionalized for different antibodies due to various antibody sizes and charges.

To confirm the validity of the sensor and sensitivity to CIP2A protein, the biofunctionalized strips were tested using pure CIP2A protein serially diluted into various concentrations beginning from pure PBS and working down to 1×10^{-15} g/ml dilution in PBS.

Figure 3 shows the sensor drain waveform as a result of increasing

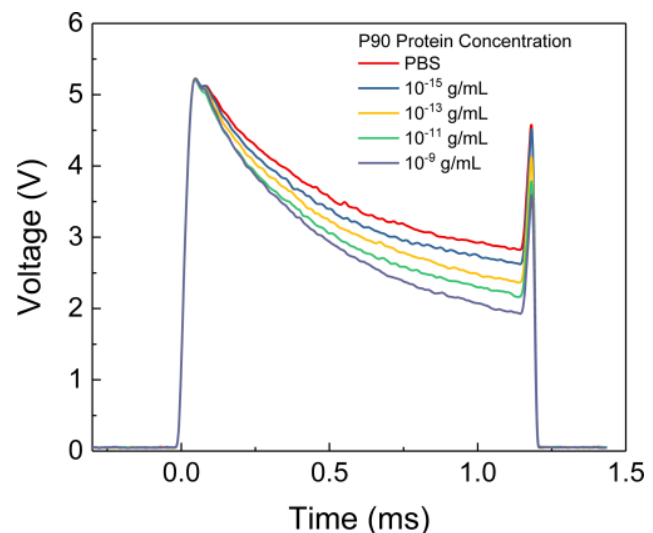


FIG. 3. Sensor waveform for pure CIP2A diluted in PBS from 10^{-9} to 10^{-15} g/ml.

CIP2A concentration. The V_D decrease with higher concentration due to sensor strip capacitance variation was explained previously.²⁰ Figure 4(a) shows the analog voltage obtained by extracting the voltage data at $750\mu\text{s}$ value of the sensor waveform, V_D reading decrease linearly for CIP2A protein concentration range from pure PBS up to $1 \times 10^{-5}\text{ g/ml}$ on a logarithmic scale. The ultimate sensitivity obtained is $1 \times 10^{-15}\text{ g/ml}$ with a sensitivity of 87 mV/dec ; these results show that such a system is at six orders of magnitude more sensitive than ELISA kits.¹⁶ The digital readings, a four-digit number, were obtained directly from the built-in LCD, and the number is translated directly from the V_D waveform via the built-in VCO and counter. Figure 4(b) shows that across the whole

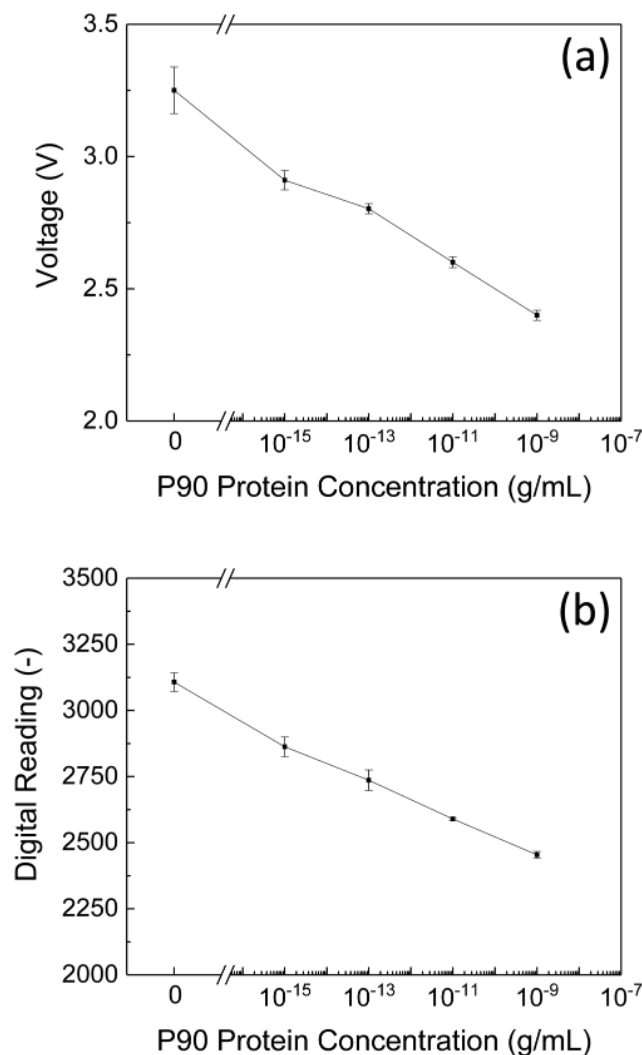


FIG. 4. Analog reading at $750\mu\text{s}$ value of sensor waveform (a) and digital sensor board output (b) from an average of ten measurements for serial dilution of CIP2A protein in PBS in the range of 10^{-9} – 10^{-15} g/ml .

concentration range tested down to $1 \times 10^{-15}\text{ g/ml}$, the output maintains a linear relationship with respect to concentration on a logarithmic scale from around 3100 to 2450, with a sensitivity of $69/\text{dec}$. The sensor has not reached saturation at the 1×10^{-5} dilution, but a higher concentration that saturates the system would not be clinically relevant.

Compared to ELISA test methods, which require lengthy processing times and lower sensitivity, a new test method using brush biopsies of potentially cancerous or suspicious lesions could offer a unique advantage to dental offices in a quick and easy sample collection process for cancer screening. Given the sensor's high sensitivity for the protein in CIP2A protein, a proven positive control from human cancer cells for CIP2A antibody can be used for testing in this case. HeLa whole-cell lysate was acquired and tested with the same setup and parameter to examine sensor functionality in the human cancer cell. It is a positive control in the western blot method for this particular antibody. Figure 5 shows the same monotonically decreasing trend when testing with sensor strips with the same functionalization steps and identical sensing parameters without further adjustment. Figure 6(a) shows that the linear analog voltage change can be directly obtained after averaging the ten sensing pulses. A net 111 mV/dec sensitivity was calculated from the analog voltage extracted from the $750\mu\text{s}$ value of the analog waveform. The direct digital output Fig. 6(b) shows a linear reduction of digital reading from about 3400 to 2350 for the concentration range from pure PBS to $1 \times 10^{-15}\text{ g/ml}$, with a digital sensitivity of $91/\text{dec}$. The exact concentration of CIP2A expressed in HeLa cell lysate is unknown. However, given that a positive detection result was obtained from a proven positive control cell lysate containing protein to be detected, this result has shown a potential detection limit beyond $1 \times 10^{-15}\text{ g/ml}$. It demonstrates the exceptional sensitivity achievable by this approach.

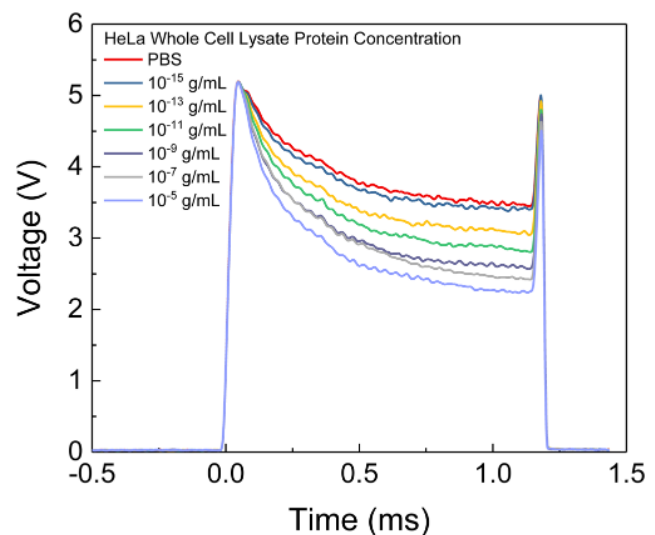


FIG. 5. Sensor waveform for human HeLa cell lysates diluted in PBS from 10^{-5} to 10^{-15} g/ml .

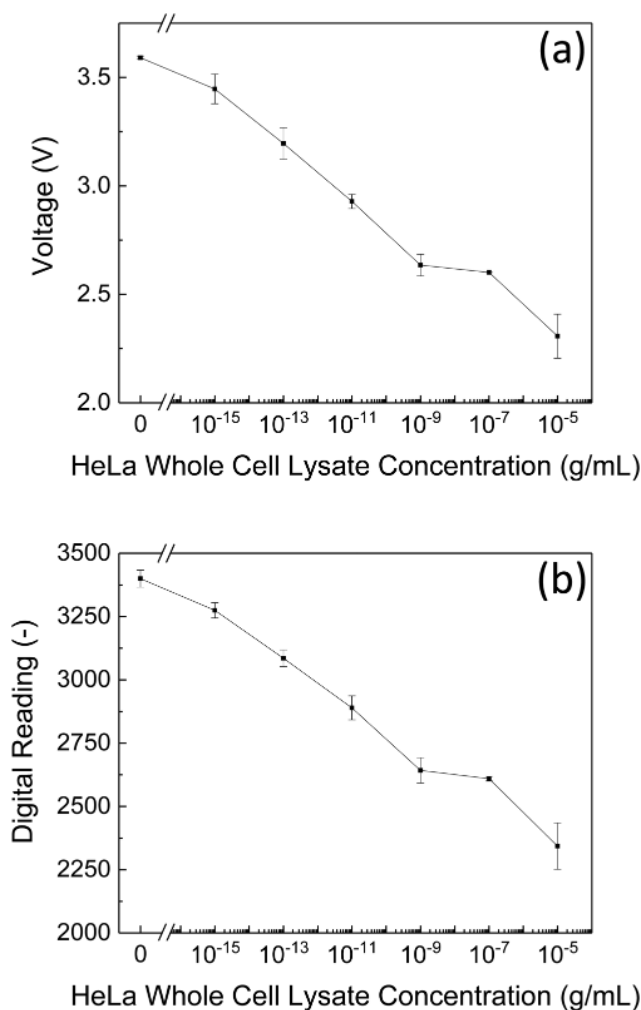


FIG. 6. Average analog reading extracted at 750 μ s value of sensor waveform (a) and average direct digital readout on circuit board from an average of 10 measurements for human HeLa cell lysates diluted in PBS from 10⁻⁵ to 10⁻¹⁵ g/ml (b).

IV. CONCLUSIONS

Transistor-based biosensor system was used and optimized for biomarker detection of the biomarker for OSCC in this work. Compared to conventional assays such as ELISA, the result using pure CIP2A protein with the optimal sensor setup shows six orders of magnitude higher sensitivity than the commercially available ELISA test kit. While subsequent testing using a cancel cell sample, human whole HeLa cell lysate showed comparable sensitivity using an identical setup. This offers an opportunity and versatility to develop a similar system for rapid, low-cost, and portable immunoassay in the medical and diagnostic sector. The next step in this continuum will be to test clinical saliva samples in oral cancer patients and determine the presence of CIP2A in saliva.

ACKNOWLEDGMENTS

The work at UF is partially supported by R01-DE025001 grant from the National Institute of Dental and Craniofacial Research (NIDCR) at The National Institutes of Health (NIH).

AUTHOR DECLARATIONS

Conflict of Interest

The authors have no conflicts to disclose.

Author Contributions

Minghan Xian: Data curation (equal); Formal analysis (equal); Investigation (equal); Writing – original draft (lead); Writing – review and editing (lead). **Jenna L. Stephany:** Data curation (equal); Formal analysis (equal); Investigation (equal); Writing – original draft (lead). **Chan-Wen Chiu:** Data curation (equal); Investigation (equal). **Chao-Ching Chiang:** Data curation (supporting); Investigation (supporting). **Fan Ren:** Resources (equal); Supervision (equal); Writing – review and editing (equal). **Cheng-Tse Tsai:** Resources (equal). **Siang-Sin Shan:** Resources (equal). **Yu-Te Liao:** Resources (equal). **Josephine F. Esquivel-Upshaw:** Resources (equal); Supervision (equal); Writing – review and editing (equal). **Stephen J. Pearton:** Supervision (equal).

DATA AVAILABILITY

The data that support the findings of this study are available from the corresponding author upon reasonable request.

REFERENCES

- ¹M. A. Kuriakose, *Contemporary Oral Oncology* (Springer International Publishing, Switzerland, 2017).
- ²M. W. Lingen, J. R. Kalmar, T. Karrison, and P. M. Speight, *Oral Oncol.* **44**, 10 (2008).
- ³A. Eftekhari, M. Hasanazadeh, S. Sharifi, S. M. Dizaj, R. Khalilov, and E. Ahmadian, *Int. J. Biol. Macromol.* **124**, 1246 (2019).
- ⁴S. Ding *et al.*, *Biosens. Bioelectron.* **117**, 68 (2018).
- ⁵J. Katz, A. Jakymiw, M. K. Ducksworth, C. M. Stewart, I. Bhattacharyya, S. Cha, and E. K. L. Chan, *Cancer Biol. Ther.* **10**, 694 (2010).
- ⁶M. R. Junttila *et al.*, *Cell* **130**, 51 (2007).
- ⁷J. R. Basile and R. Czerninski, *Cancer Biol. Ther.* **10**, 700 (2010).
- ⁸B. K. Velmurugan, H. K. Wang, C. M. Chung, C. H. Lee, L. R. Huang, K. T. Yeh, and S. H. Lin, *Cancer Manag. Res.* **11**, 2589 (2019).
- ⁹Y. C. Lin, K. C. Chen, C. C. Chen, A. L. Cheng, and K. F. Chen, *Oral Oncol.* **48**, 585 (2012).
- ¹⁰B. Peng, Y. Chai, Y. Li, X. Liu, and J. Zhang, *BMC Cancer* **15**, 1 (2015).
- ¹¹C. Böckelman, J. Hagström, L. K. Mäkinen, H. Keski-Säntti, V. Häyry, J. Lundin, T. Atula, A. Ristimäki, and C. Haglund, *Br. J. Cancer* **104**, 1890 (2011).
- ¹²X. D. Chen, S. X. Tang, J. H. Zhang, L. T. Zhang, and Y. W. Wang, *Oncol. Rep.* **38**, 1005 (2017).
- ¹³Y. T. Lin, S. Darvishi, A. Preet, T. Y. Huang, S. H. Lin, H. H. Girault, L. Wang, and T. E. Lin, *Chemosensors* **8**, 54 (2020).
- ¹⁴J. Routila, T. Bilgen, O. Saramäki, R. Grénman, T. Visakorpi, J. Westermarck, and S. Ventelä, *J. Oral Pathol. Med.* **45**, 329 (2016).
- ¹⁵M. Seppälä, S. Tervo, K. Pohjola, J. Laranne, H. Huhtala, S. Toppila-Salmi, and T. Paavonen, *APMIS* **123**, 1007 (2015).
- ¹⁶MyBioSource.Com.: KIAA1524 Elisa Kit Hum. Cancerous Inhib. PP2A ELISA Kit (2022).

- ¹⁷M. Xian, P. H. Carey, C. Fares, F. Ren, S. S. Shan, Y. Te Liao, J. F. Esquivel-Upshaw, and S. J. Pearton, in *2020 IEEE Research and Applications of Photonics in Defense Conference RAPID 2020—Proceedings*, Virtual format, 12 August 2020, (IEEE, New York, 2020).
- ¹⁸M. Xian *et al.*, *J. Vac. Sci. Technol. B* **39**, 033202 (2021).
- ¹⁹C.-W. Chiu *et al.*, *J. Vac. Sci. Technol. B* **40**, 023204 (2022).
- ²⁰M. Xian *et al.*, *J. Vac. Sci. Technol. B* **40**, 023202 (2022).
- ²¹P. H. Carey *et al.*, *J. Electrochem. Soc.* **167**, 037507 (2020).
- ²²J. Yang, P. Carey, F. Ren, M. A. Mastro, K. Beers, S. J. Pearton, and I. I. Kravchenko, *Appl. Phys. Lett.* **113**, 032101 (2018).
- ²³S.-S. Shan *et al.*, *IEEE Trans. Biomed. Circuits Syst.* **14**, 1362 (2020).
- ²⁴B. S. Kang, F. Ren, Y. W. Heo, L. C. Tien, D. P. Norton, and S. J. Pearton, *Appl. Phys. Lett.* **86**, 112105 (2005).
- ²⁵B. S. Kang *et al.*, *Appl. Phys. Lett.* **89**, 122102 (2006).
- ²⁶T. J. Anderson, K. D. Hobart, M. J. Tadjer, A. D. Koehler, T. I. Feygelson, B. B. Pate, J. K. Hite, F. J. Kub, and C. R. Eddy, *ECS Trans.* **64**, 185 (2014).
- ²⁷D. R. Hekstra, K. I. White, M. A. Socolich, R. W. Henning, V. Šrajer, and R. Ranganathan, *Nature* **540**, 400 (2016).
- ²⁸M. Hamdi, G. Sharma, A. Ferreira, and C. Mavroidis, in *Proceedings of the IEEE International Conference on Robotics and Automation*, Orlando, FL, 15–19 May 2006, (IEEE, New York, 2006), Vol. 2006, p. 1794.